

Discussions on Chiral symmetry from Roy equation analysis

郑汉青

四川大学

2026 年 4 月 24 日

第八届重味物理与 QCD 会议，重庆大学，2026.4.25-4.28

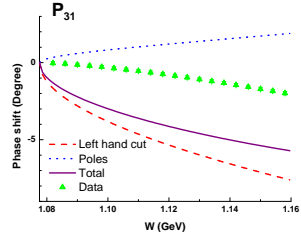
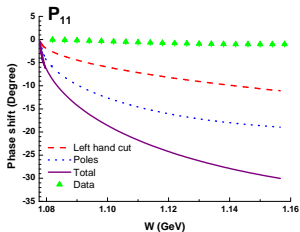
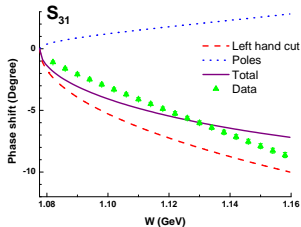
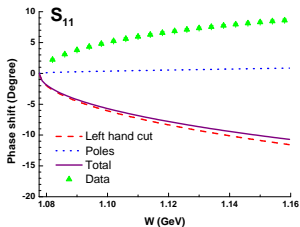
CONTENTS

- 1 πN scatterings and $N^*(920)$
 - PKU representation
 - Roy-Steiner equation analysis
- 2 $\pi\pi$ phase shift at un-physical pion masses
- 3 Temperature and Density

LOW ENERGY πN SCATTERING PHASE SHIFTS

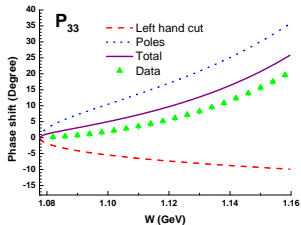
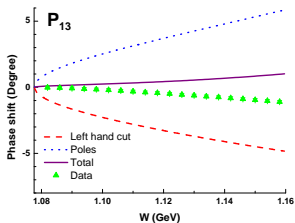
Estimated both at $O(p^2)$ and $O(p^3)$ level. (Tree level plotted). $L_{2I 2J}$ convention, $W = \sqrt{s}$, data: green

triangles [SAID: WI 08]



LOW ENERGY πN SCATTERING PHASE SHIFTS

$L_{2I 2J}$ convention, $W = \sqrt{s}$, data: green triangles [SAID: WI 08]

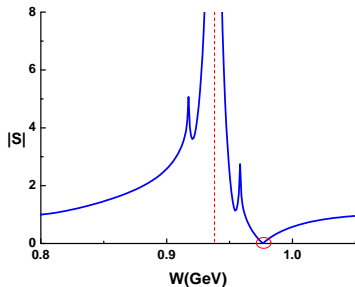


DISCREPANCIES IN S_{11} AND P_{11} CHANNELS

Large missing positive contributions

P_{11} :

- Analytical continuation: $S^{\text{II}} = 1/S^{\text{I}}$.
Second sheet poles \rightarrow first sheet zeros.
- Expansion: $S^{\text{I}} \sim a/(s - M_N^2) + b + \dots$
- Arbitrary non-zero $b \rightarrow$ the virtual state
- Perturbation calculation \rightarrow virtual state at 976 MeV; fit \rightarrow 980 MeV



FINDING S_{11} HIDDEN POLE

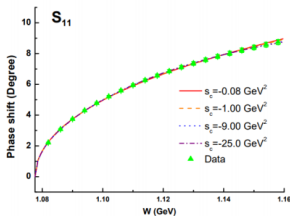
$O(p^2)$ [YF Wang et al., 2018 EPJC];

$O(p^3)$ [YF Wang et al., 2019 CPC]

- Hidden pole \rightarrow a “crazy resonance” below threshold $0.895(81)(2) - 0.164(23)(4)i$ GeV.

s_c (GeV ²)	Pole position (MeV)	$\chi^2/\text{d.o.f}$
-0.08	$814(3) - i 141(8)$	1.46
-1.00	$882(2) - i 190(4)$	1.31
-9.00	$960(2) - i 192(2)$	1.14
-25.0	$976(2) - i 187(1)$	1.14

Table 2: The S_{11} hidden pole fit with different choices of s_c .



PKU REPRESENTATION

- Production representation, or PKU representation: elastic two-body scattering amplitude

$$S = \prod_i S_i \times S_{cut}$$

- S_i : pole terms, $S_{cut} = e^{2i\rho(s)f(s)}$: left-hand cuts and right hand inelastic cut – background.

$$f(s) = \frac{s}{2\pi i} \int_L ds' \frac{\text{disc}f(s')}{(s' - s)s'} + \frac{s}{2\pi i} \int_{R'} ds' \frac{\text{disc}f(s')}{(s' - s)s'}$$

- $f(0) \equiv 0$ [Z. Y. Zhou and H. Q. Zheng 2006 NPA]

QFT version of Ning Hu representation



Prof. Ning Hu (1916–1997)

- 1943: PhD in Caltech.
- 1942–1945: IAS, Princeton.
- 1945–1947: IAS, Ireland.
- 1947 – 1948: Nils Bohr Institute.
- 1948 – 1950, Cornell U., Wisconsin U..
- 1951 – 1997: Peking University

Theory for meson nucleon interaction;
General relativity and gravitational wave;
 S matrix theory;
Quantum electro dynamics;
Quark model.

Roy-Steiner equation

Roy-Steiner Equation

[Roy 1971]

- A coupled system of PWDRs.
- Analyticity, Unitarity, and Crossing symmetry.

Starting from the twice-subtracted fixed- t dispersion relation:

$$T(s, t, u) = \alpha(t) + s\beta(t) + \frac{s^2}{\pi} \int_{4m_\pi^2}^{\infty} ds' \frac{\text{Im } T(s', t, u')}{s'^2 (s' - s)} + \frac{s^2}{\pi} \int_{-\infty}^{-t} ds' \frac{\text{Im } T(s', t, u')}{s'^2 (s' - s)}, \quad (1)$$

A system of integral equations for the $\pi\pi$ amplitudes:

$$\text{Re } t_J^I(s) = k_J^I(s) + \sum_{I'} \sum_{J'} \int_{4m_\pi^2}^{\infty} ds' K_{JJ'}^{II'}(s', s) \text{Im } t_{J'}^{I'}(s'). \quad (2)$$

- $K_{JJ'}^{II'}(s', s)$: Analytically calculable kinematic kernel functions.
- The only free parameters: S -wave scattering lengths a_0^0, a_0^2 .

An important issue is the range of validity of the Roy equations.

Roy-Steiner equation



Shasanka Mohan Roy **Frank Steiner**

Lehmann ellipse constraints

$$\text{Im}_s T(s', t) = 16\pi \sum_l (2l+1) \text{Im}_s T_l(s') P_l(z(s', t)) , \quad (3)$$

z : **CMS scattering angle cosines.**

The series of Legendre polynomials converges when z within the corresponding large Lehmann ellipses [Lehmann 1958].

Lehmann ellipses

- Focal points: $z = \pm 1$.
- Boundary: Touching the nearest singularity of $\text{Im}_s T(s', t)$.

Assuming that the scattering amplitude satisfies Mandelstam's double spectral representation.

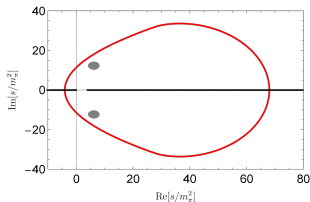


Figure: Domain of validity of the Roy Equation; black points denote the $\sigma(f_0(500))$.

Similarly, for πK and πN scattering amplitudes:

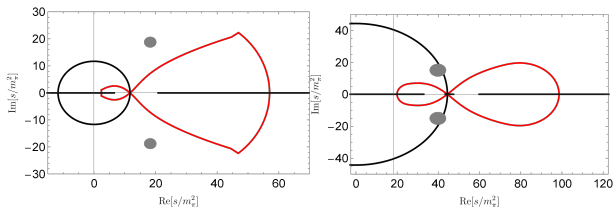


Figure: Left: πK systems, points denote the $\kappa(K_0^*(700))$; Right: πN systems, points denote the $N^*(890)$

Roy equation (fixed- t dispersion relation): unfit to search for a wide resonance.

Using the hyperbolic dispersion relations, One can get the Roy-Steiner equations, which looks like:

$$\begin{aligned} \operatorname{Re} f_l(s) &= N_l(s) + \sum_{l'} \int_{s_{th}} ds' K_{l,l'}(s, s') \operatorname{Im} f_l(s') + \sum_J \int_{t_{th}} dt' G_{l,J}(s, t') \operatorname{Im} g(t')_J, \\ \operatorname{Re} g_J(t) &= \tilde{N}_J(t) + \sum_{l'} \int_{s_{th}} ds' \tilde{K}_{J,l'}(t, s') \operatorname{Im} f_l(s') + \sum_{J'} \int_{t_{th}} dt' \tilde{G}_{J,J'}(t, t') \operatorname{Im} g(t')_{J'}. \end{aligned} \quad (4)$$

- $f_l(s)$: s-channel PWAs;
- $g_J(t)$: t-channel PWAs;
- N, K, G : Analytically calculable kinematic kernel functions.

RS equation analysis of πN scatterings

RS equation has been applied to study πN scatterings [Ditsche:2012, Hoferichter:2015].

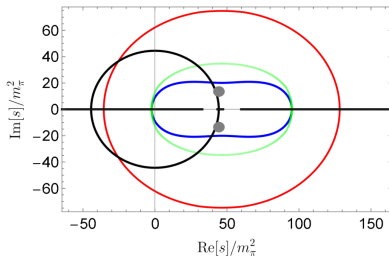


FIG. 2: Validity domain of the fixed- b RS representation ($a = 0$). The blue and green lines correspond to the boundaries in the s' and t' integrals associated with ρ_{st} , respectively. The red line corresponds to the boundaries in the s' integral associated with ρ_{su} .

[Cao XH, Li QZ, HQZ, JHEP 12 (2022) 073].

- S_{11} : $\sqrt{s} = 919 \pm 4 - (162 \pm 7)i$ $N^*(920)$.
- P_{33} : $\sqrt{s} = 1213 \pm 2 - (50 \pm 3)i$ $\Delta(1232)$.

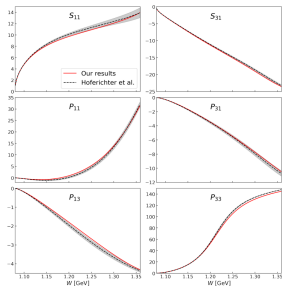
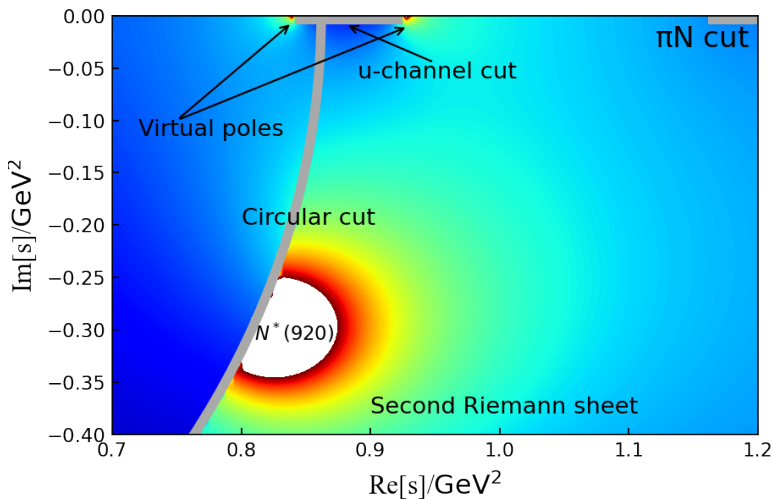
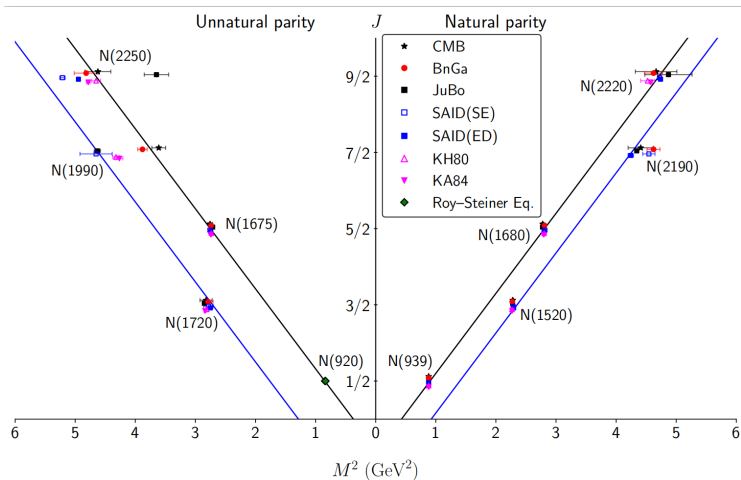


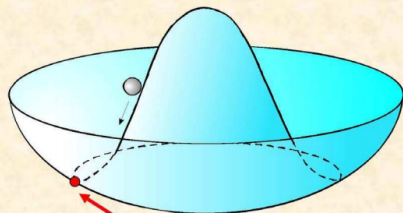
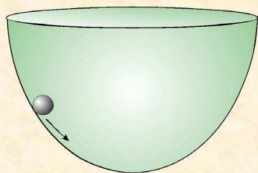
FIG. 3: Phase shifts of the s -channel PWs from our solutions (solid line) and [10] (dashed line with error bands) in the low-energy region. The deviation of P_{33} phase shift comes from the difference between values of GWU/SAID and [10] at the matching point ($W_m = 1.36$ GeV), and they differ by about 2° .



Regge Trajectory



Ground State – Vacuum



Chiral symmetry breaking



M.R. Pennington, YKIS06

The linear sigma model

The linear sigma model

$$\begin{aligned}\mathcal{L} &= \mathcal{L}_s + c\sigma, \\ \mathcal{L}_s &= \frac{1}{2}[(\partial_\mu\sigma)^2 + (\partial_\mu\pi)^2] + \frac{m^2}{2}[\sigma^2 + \pi^2] - \frac{\lambda}{4}[\sigma^2 + \pi^2]^2, \quad (1)\end{aligned}$$

when $c \rightarrow 0$, the lagrangian is invariant under $SU_L(2) \times SU_R(2)$ chiral rotations

$$\begin{aligned}\vec{\pi} &\rightarrow \vec{\pi} + \vec{\alpha} \times \vec{\pi} - \vec{\beta}\sigma, \\ \sigma &\rightarrow \sigma + \vec{\beta} \cdot \vec{\pi}\end{aligned} \quad (2)$$

Weinberg's
"Folk Theorem"



If one writes down the most general possible Lagrangian, including all terms consistent with assumed symmetry principles, and then calculates matrix elements with this Lagrangian to any given order of perturbation theory, the result will simply be the most general possible S -matrix consistent with analyticity, perturbative unitarity, cluster decomposition, and the assumed symmetry principles.

Physica **96A**, 327 (1979)

To be or not to be, this is a question

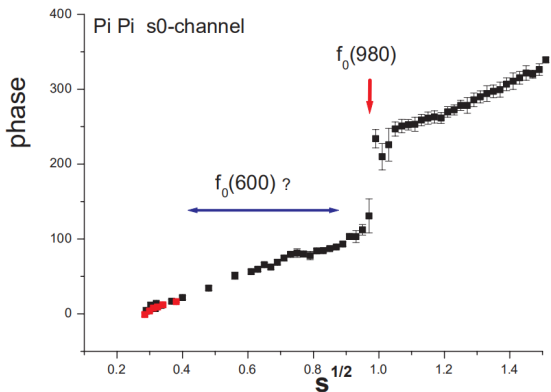
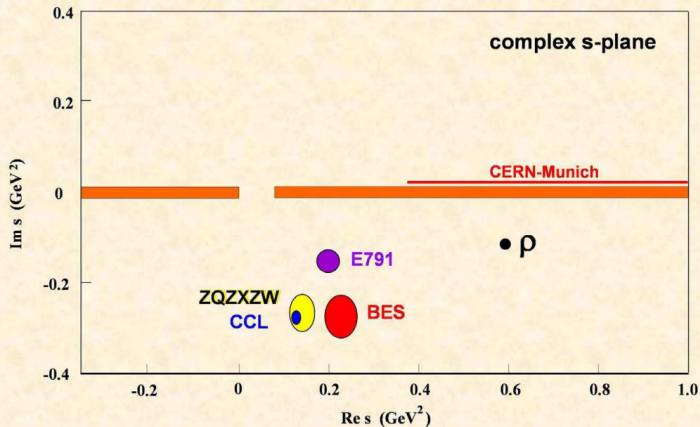


Figure: $IJ=00$ channel $\pi\pi$ scattering phase shift data from CERN-Munich and E865.

$$\pi\pi : I = 0, J = 0$$



Zhou, Qin, Zhang, Xiao, Zheng & Wu

Caprini, Colangelo, & Leutwyler

M.R. Pennington, YKIS06

$\pi\pi$ phase shift at un-physical pion masses

[Cao XH, Li QZ, Guo ZH, HQZ, Phys.Rev.D 108 (2023) 3, 034009]

Modified Roy equations; Lattice data

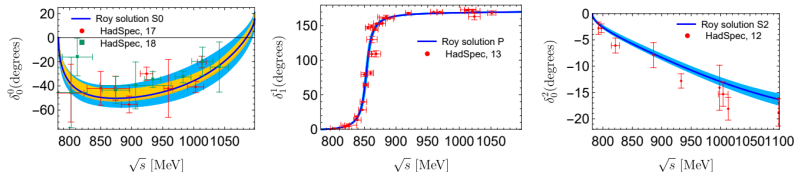


FIG. 6. $\pi\pi$ phase shifts at $m_\pi = 391$ MeV from Roy equation solutions: S0, P and S2 stand for the results of the $IJ = 00, 11, 20$ channels, respectively. For the sources of the shaded error bands, see the main text for details. The lattice data are taken from Refs. [24–26, 28].

$$a_0^0 = -(3.8^{+1.1}_{-1.2}), \quad a_0^2 = -(0.21^{+0.02}_{-0.03}),$$

$$\sqrt{s_\sigma} = 759^{+7}_{-16} \text{ MeV}, \quad |g_{\sigma\pi\pi}| = 493^{+27}_{-46} \text{ MeV}.$$

$\pi\pi$ phase shift at un-physical pion masses

[Cao XH, Li QZ, Guo ZH, HQZ, Phys.Rev.D 108 (2023) 3, 034009

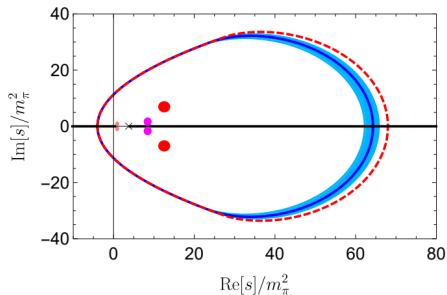


FIG. 7. Validity domain of extended Roy equation for $m_\pi = 391$ MeV. The dashed red boundary represents the validity domain by dropping the effects of the bound state σ , and the blue boundary corresponds to the complete validity domain within uncertainty from the location of the σ . The poles in the validity domain in the second RS are from left to right, as shown in Eq. (15).

$\pi\pi$ phase shift at un-physical pion masses

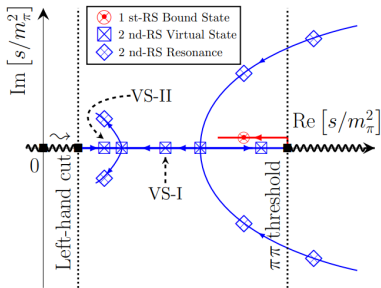


FIG. 9. The qualitative trajectory of the σ pole on the second RS of the s plane with varying m_π . See the main text for the meaning of the labels ‘VS-I,II’.

O(N) σ model revisited at different pion masses

[Lyu YL, Li QZ, Xiao ZG, HQZ, Phys.Rev.D 109 (2024) 9, 094026; ibid 110 (2024) 9, 094054]

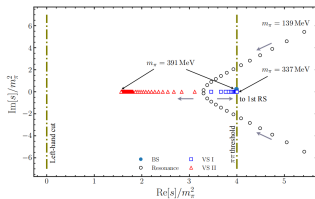


Figure: Large N method. Pole position with respect to different m_π .

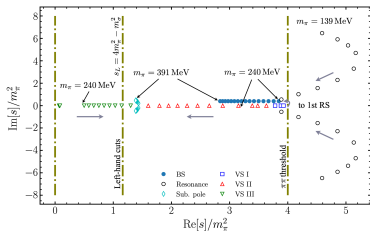


Figure: N/D improved. Pole position with respect to different m_π .

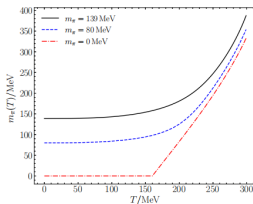
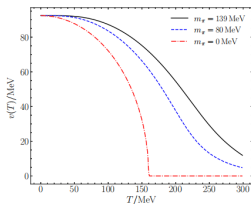
O(N) σ model revisited at different temperatures

- The leading order effective potential at finite temperature T can be obtained with imaginary time formalism [M. L. Bellac, *Thermal Field Theory*, CUP 2011] by Wick rotation to Euclidean space and substituting the momentum integral with a sum over Matsubara frequencies $\omega_n = 2\pi nT$, i.e. $\int \frac{d^4k}{(2\pi)^4} f(k_0, \mathbf{k}) \rightarrow iT \sum_n \int \frac{d^3\mathbf{k}}{(2\pi)^3} f(k_0 = i\omega_n, \mathbf{k})$.
- By minimizing the effective potential, we can obtain the gap equations for v and m_π^2 as functions of temperature [J. O. Andersen, D. Boer, and H. J. Warringa, PRD 2004] :

$$v^2(T) = f_\pi^2 + \frac{N}{16\pi^2} \left(m_\pi^2 \log \frac{m_\pi^2}{M^2} - m_\pi^2(T) \log \frac{m_\pi^2(T)}{M^2} \right) - NA^{T \neq 0} (m_\pi^2(T), T)$$

$$\alpha = v(T) m_\pi^2(T)$$

where $v(0) = f_\pi$ and $m_\pi(0) = m_\pi$ are set to zero-temperature values.



$O(N)$ σ model revisited at different temperatures

- The $I = J = 0$ channel scattering amplitude at LO $1/N$ expansion with finite temperature is obtained as,

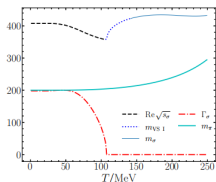
$$\mathcal{T}_{00}^T(s) = -\frac{1}{32\pi} \frac{s - m_\pi^2(T)}{(s - m_\pi^2(T)) B^T(s, m_\pi(T), M) - v^2(T)/N},$$

where the finite temperature effect introduced by loop diagrams can be standardly calculated as

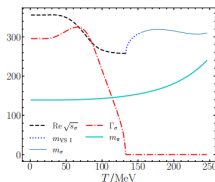
$$B^T(s, m_\pi(T), M) = B(s, m_\pi(T), M) + B^{T \neq 0}(s, m_\pi(T), T),$$

$$B^{T \neq 0}(s, m_\pi(T), T) = \int_0^\infty \frac{dk k^2}{8\pi^2 \omega_k^2} n_B(\omega_k) \left(\frac{1}{E + 2\omega_k} - \frac{1}{E - 2\omega_k} \right),$$

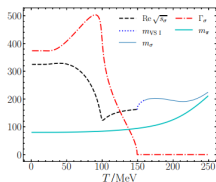
with $\beta = 1/T$, $\omega_k = \sqrt{k^2 + m_\pi^2(T)}$ and $n_B(\omega_k) = (e^{\beta\omega_k} - 1)^{-1}$ is the Bose-Einstein distribution. $B^{T \neq 0}$ is evaluated in the CM frame and $s = E^2$.



$m_\pi = 200$ MeV



$m_\pi = 139$ MeV



$m_\pi = 80$ MeV

N/D improved calculations

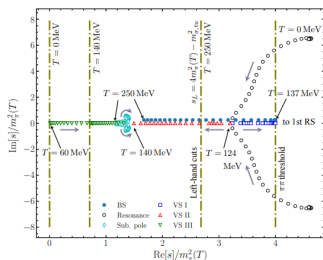
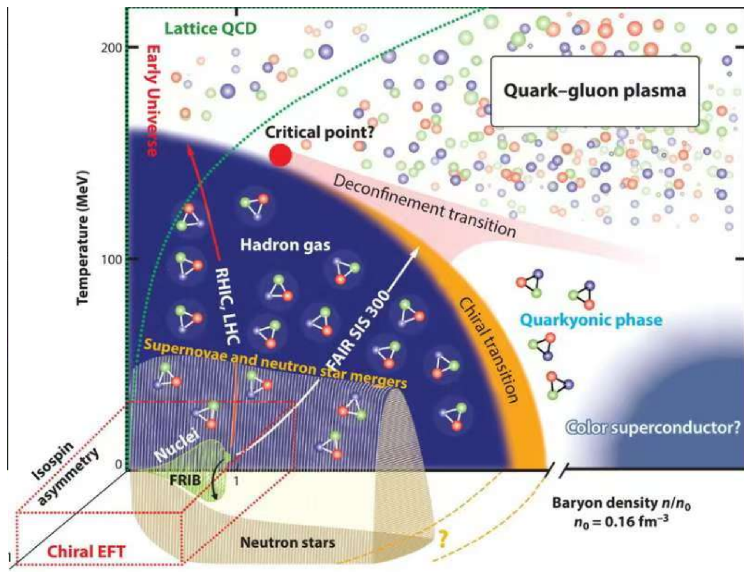


FIG. 16. The thermal σ pole trajectory obtained in N/D modified $O(N)$ model. The zero-temperature pion mass is set as $m_\pi(0) = 139$ MeV. When the temperature increases, similar to the leading order result [18], σ turns into two virtual states (VS I&II) and then becomes a bound state (BS) after VS I moves towards and across the threshold to the first Riemann sheet (RS). The left-hand cut branch point extends to $s_L = 4m_\pi^2(T) - m_{\sigma,tu}^2$ due to the σ exchange in crossed channels. Additionally, the third virtual state pole (VS III) generated close to s_L will meet VS II on the real axis, then becoming a pair of subthreshold (Sub.) poles and going into the complex plane. Finally, the pair of subthreshold poles tends to $s_A = m_\pi^2(T)$ as $T \gg T_c$.

Temperature properties of $N^*(920)$



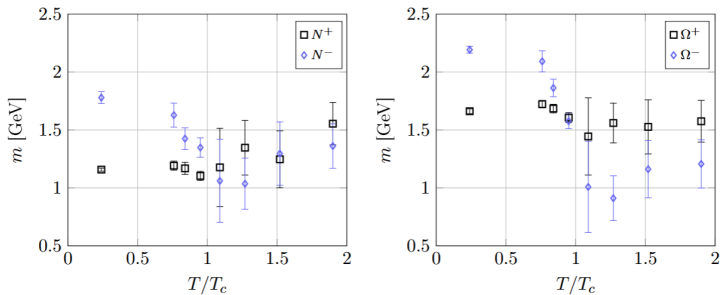


Figure 3. Groundstate masses in the positive- and negative-parity channels at *all* temperatures, assuming the exponential decay of Eq. (4.2), in the N (left) and Ω (right) channels.

$T_c = 185\text{MeV}$; [G. Aarts et al., JHEP 06 (2017)]

$N^*(920)$?!

Spontaneous symmetry breaking

If the ground state of QCD (=hadron spectrum) has the same symmetry as the Lagrangian (namely, chiral symmetry), then “parity doublets” exist; because:

Let $|i, +\rangle$ denote an eigenstate of H_{QCD}^0 with eigenvalue E_i ,

$$H_{\text{QCD}}^0|i, +\rangle = E_i|i, +\rangle,$$

having positive parity,

$$P|i, +\rangle = +|i, +\rangle,$$

such as, e.g., a member of the ground state baryon octet (in the chiral limit).

Defining $|\phi\rangle = Q_A^a|i, +\rangle$, because of $[H_{\text{QCD}}^0, Q_A^a] = 0$, we have

$$H_{\text{QCD}}^0|\phi\rangle = H_{\text{QCD}}^0 Q_A^a|i, +\rangle = Q_A^a H_{\text{QCD}}^0|i, +\rangle = E_i Q_A^a|i, +\rangle = E_i|\phi\rangle,$$

i.e., the new state $|\phi\rangle$ is also an eigenstate of H_{QCD}^0 with the same eigenvalue E_i but of opposite parity:

$$P|\phi\rangle = P Q_A^a P^{-1} P|i, +\rangle = -Q_A^a(+|i, +\rangle) = -|\phi\rangle.$$

Spontaneous symmetry breaking, cont'd

What would parity doublets look like?

Nucleons of positive parity: $p(1/2^+, 938.3)$, $n(1/2^+, 939.6)$, $I=1/2$;

nucleons of negative parity: $N(1/2^-, 1535)$, $I=1/2$.

But, the masses are very different: **NOT** a parity doublet!

A meson of negative parity: $\rho(1^-, 770)$, $I=1$,

the "same" with positive parity: $a_1(1^+, 1260)$, $I=1$.

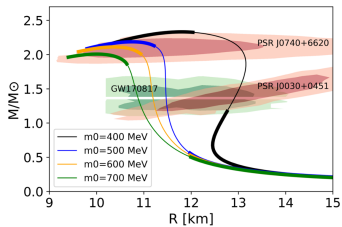
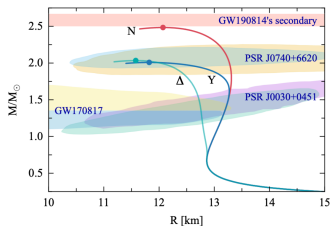
But again, the masses are very different: **NOT** a parity doublet!

Conclusion: Parity doublets are **not** observed in the low-energy hadron spectrum.



Chiral symmetry is spontaneously broken.

Neutron Star



[T. Minamikawa, B. Gao, T. Kojo, and M. Harada, *Symmetry* 15, 745 (2023)]

Conclusions and Perspectives

- 1 There exists a spin one half, negative parity sub-threshold nucleon pole.
- 2 σ becomes a bound state pole at large m_π and high temperature.
- 3 Parity doublet model!? EOS Neutron star?

Final goals: fully understanding the role of $N^*(920)$

— Thanks for patience!